SOME ASPECTS OF THE HIGH-TEMPERATURE BEHAVIOUR OF AN IN SITU Ti-Ti_5Si_3 EUTECTIC COMPOSITE

DALIBOR VOJTĚCH[1]*, HANA ČÍŽOVÁ[1], JAROSLAV MAIXNER[2]

[1]*Department of Metals and Corrosion Engineering, Institute of Chemical Technology, Technická 5, 166 28 Prague 6, Czech Republic*
[2]*Laboratory of X-ray Diffraction, Institute of Chemical Technology, Technická 5, 166 28 Prague 6, Czech Republic*

Received 5 January 2005, accepted 1 March 2005

The work describes some aspects of the high-temperature behaviour of an in situ Ti-Ti_5Si_3 eutectic composite at 750–1050 °C. The alloy was annealed under vacuum and its changes induced by high-temperature expositions were monitored using a microstructural examination, XRD and hardness measurement. The cyclic oxidation was conducted in CO_2 for 108 hours, and its kinetics was investigated by the way of weight gains measurements and by a detailed examination of the scales. The in situ Ti-Ti_5Si_3 eutectic composite was found to correspond to the as-cast TiSi8 (in wt.%) alloy. The Ti_3Si phase was not found in the as-cast state due to the kinetic factor and the presence of carbon. The high-temperature exposition at 750–850 °C induced slow coarsening of the eutectic Ti_5Si_3 silicide and its precipitation from a supersaturated solid solution. No phase transformation, e.g. into Ti_3Si, was detected, which was consistent with the stabilizing effect of carbon. The structural changes were accompanied with a very slow hardness reduction. The measurements of the oxidation kinetics and its comparison with pure Ti proved a strong protecting effect of the Ti_5Si_3 silicide at 850–1050 °C. The slow oxidation of Ti-Ti_5Si_3 at 850–950 °C was governed by diffusion through the scales, and was described by the parabolic law. On the other hand, pure Ti and the Ti-Ti_5Si_3 alloy oxidized at 1050 °C did not obey the parabolic law due to the scales porosity, cracking, and poor adherence to the substrate. The WDS and XRD analyses proved that the main component of the scales on both pure Ti and the Ti-Ti_5Si_3 alloy was rutile. The scales on the Ti-Ti_5Si_3 alloy also contained amorphous silica with a small amount of carbon. Silica, which was responsible for a strong oxidation rate reduction, originated from the oxidation of the Ti_5Si_3 silicide.

K e y w o r d s: titanium, titanium silicide, high-temperature material, metal matrix composite, high-temperature oxidation, eutectic

*corresponding author, e-mail: Dalibor.Vojtech@vscht.cz

1. Introduction

Titanium alloys attract considerable interest of materials engineers due to their excellent combination of strength, low density and corrosion resistance. Commercially available titanium-based alloys designed for elevated temperature applications in the aerospace and automotive industries are known as "near-α alloys". Besides aluminium and tin, these alloys contain thermally stabilizing elements such as Zr, Mo and Si. Silicon is believed to precipitate at high temperatures on dislocations, thus hindering their movement and improving creep resistance. Generally, silicon concentrations in these alloys do not exceed a few tenths of weight percent. An example of a "near-α" alloy is the Ti-6-2-4-2-Si alloy containing 6 wt.% Al, 2 wt.% Sn, 4 wt.% Zr, 2 wt.% Mo and 0.1 wt.% Si [1]. The "near-α" alloys are characterized by good chemical and creep resistance at elevated temperatures, with their maximum service temperatures being close to 600 °C. For higher temperatures (above 700 °C), however, these alloys are insufficient. For structural components in the aerospace and automotive industries, which are exposed to high temperatures (e.g. turbine blades, turbine wheels, exhaust valves etc.), γ-(TiAl)-based alloys have been developed [2–4]. At temperatures between 600–800 °C, the specific strength of these alloys is superior to that of the "near-α" alloys and similar to Ni-based alloys.

Another way of improving the high-temperature mechanical properties of Ti-based alloys is their reinforcement with hard ceramic fibres or particles, i.e. formation of metal matrix composites (MMCs) [5]. Eutectic alloys can be regarded as "in situ" MMCs, as the reinforcement is formed directly upon cooling by a eutectic reaction. In addition, reinforcing carbides and silicides are also known to be both thermally and in particular chemically very stable phases. Their excellent high-temperature oxidation resistance is attributed to the protective silica layer in the scales. This work is focused on the Ti-Ti_5Si_3 system in which the silicide phase is formed in situ directly by a eutectic reaction from the melt.

The equilibrium phase diagram of the Ti-Si system is shown in Fig. 1. It can be seen that there is a relatively deep eutectic at 8.5 wt.% Si and 1330 °C. The eutectic mixture of β(Ti) + Ti_5Si_3 solidifies upon cooling of melts with a Si concentration above 3 wt.%. According to the Ti-Si phase diagram, the Ti_5Si_3 silicide should transform to the Ti_3Si phase through a peritectoid reaction at 1170 °C. However, the Ti_3Si silicide is not generally observed in as-cast Ti-Si alloys [7–9]. Instead, the Ti_5Si_3 silicide with a congruent melting point of more than 2000 °C is found most often. In addition, older publications containing the phase equilibrium data of this system [10] described only the Ti_5Si_3 phase at Si concentrations below 25 wt.% Si.

It is not surprising that the Ti_5Si_3 phase determines the majority of properties which are of interest to materials engineers. The increase in hardness and the wear and creep resistance is directly related to the growing fraction of hard silicides as the silicon concentration rises [7, 11–13]. On the other hand, strength as the principal

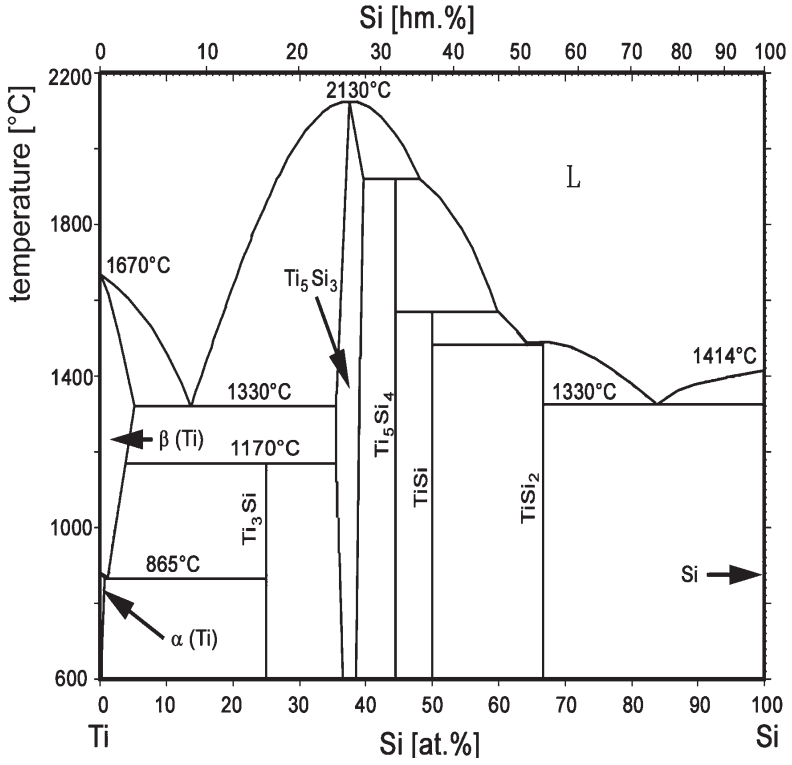

Fig. 1. Ti-Si equilibrium phase diagram [6].

mechanical characteristic is determined by a number of structural features, and it is thus far from simple to predict its value based solely on the silicide content. Strength in the as-cast state as a function of Si-concentration (0–2.75 wt.%) was measured by Zhu et al. [7]. It was found to reach its maximum at a silicon concentration of 1.8 wt.% (more than 1000 MPa), while reducing rapidly at higher concentrations. The plasticity of the TiSi1.8 alloy also exhibited a relatively good level of 7 %. The high strength is attributed to the refinement of grains by Si, and to the large volume fraction of silicides, which, however, do not form a continuous network yet. The formation of a network along the grain boundaries significantly reduces both strength and plasticity. As stated above, the Ti-Si alloys containing more than about 3 wt.% Si comprise a eutectic in the microstructure. These alloys have been investigated by a number of authors but most of them concentrated on rapidly solidified structures [14–16] because a deep eutectic promotes the formation of the amorphous phase. For the study of eutectic composites, however, properties

of as-cast alloys are important. Saha [8] studied the influence of small additions of bismuth, as a modifier of eutectic silicides, on the structure and mechanical properties of an as-cast alloy containing 6.5 wt.% Si. He found remarkably high values of tensile strength (above 800 MPa) and elongation (almost 2 %) for the alloy modified with Bi. Given the high volume fraction of a brittle silicide, the obtained value of elongation is rather surprising.

Besides mechanical properties, the oxidation resistance is of great importance when designing mechanically and thermally loaded parts. Generally, silicon is known to strongly reduce the oxidation rate of titanium. It is believed that silicon present in the surface oxide layer reduces the diffusion rate of oxygen through this layer, and it also reduces the depth of oxygen penetration into the metallic substrate. Fine silica particles present in the oxide layer also suppress the recrystallization and stratification of rutile, thus contributing to the formation of a compact layer with a low porosity. Moreover, oxidation experiments carried out in air usually reveal the synergic effect of silicon and nitrogen [17–20]. It is believed that the occurrence of a nitride, which is commonly found beneath the oxide layer [20], is closely related to the presence of silicon in an alloy. Silicon, which reduces solubility and the depth of oxygen and nitrogen penetration in titanium [18], promotes the formation of a nitride layer instead of an interstitial solid solution. The nitride particles occupy the sites where a reaction of titanium with oxygen may occur, thus slowing down the oxidation.

The aim of this work is to describe the high-temperature behaviour of an in situ Ti-Ti_5Si_3 eutectic composite at 750–1050 °C. Microstructure, phase composition, hardness, as well as oxidation behaviour of the eutectic alloy is investigated.

2. Experimental

In our experiment, a Ti-Ti_5Si_3 alloy with a nominal composition of TiSi8 (in wt.%) was investigated. The alloy was prepared by melting titanium (purity 99.9 %) and silicon (purity 99.9 %) in a graphite crucible under vacuum in an induction furnace. The total mass of the charge was 200 g. The induction heating ensured rapid melting of the charge and homogenization of the melt. The length of the melting period was 6 min and the pouring temperature was 1610 °C. Afterwards, rod-shaped castings (length 75 mm and diameter 8 mm) were prepared by centrifugal casting into a lost wax mould. The high-temperature oxidation behaviour of the Ti-Ti_5Si_3 alloy was compared with that of pure titanium (purity 99.6 %). The chemical composition of both materials is given in Table 1.

Cylinder-shaped samples of the Ti-Ti_5Si_3 alloy (8 mm in diameter and 5 mm in length) were cut directly from the castings. The microstructure, phase composition and Vickers hardness HV 5 of the alloy in the as-cast state as well as after annealing (750–850 °C, 150 h) under vacuum was studied using optical microscopy (Olympus PMEU with image analyser Lucia) and XRD (X'Pert Philips). Prior to

Table 1. Chemical composition of the investigated materials [wt.%]

Alloy	Ti	Si	C	O	S	Al	V	Fe	Cr	Mo
Ti	99.60	–	0.03	0.10	0.02	0.01	0.01	0.15	0.01	0.01
Ti-Ti_5Si_3	91.16	7.79	0.39	0.10	0.02	0.04	0.01	0.01	0.01	0.02

annealing, the samples were encapsulated into a silica glass tube, which was then evacuated and sealed. The samples for a metallographic examination were ground with SiC paper and polished with cloth and 1 micron diamond paste. The etching was performed using a mixture of 5 ml HF, 20 ml HNO_3 and 75 ml H_2O.

In our work, we used cyclic oxidation experiments to measure the oxidation resistance of the eutectic alloy. These experiments included high-temperature oxidation periods and cooling periods, and they were assumed to better simulate the real conditions of thermally loaded parts. Oxidation tests were conducted on the as-cast Ti-Ti_5Si_3 alloy and pure Ti at 850–1050 ℃. The cylindrical samples (8 mm in diameter and 5 mm in length) were cut from the castings and from an annealed Ti bar. Prior to oxidation, the surface of the samples was polished using finally 1 micron diamond paste. Oxidation was conducted in a resistance furnace in a slow flow of carbon dioxide (purity 99.0 %, flow rate 10 ml/min). The total oxidation time, which included nine cycles, was 108 h. Each cycle consisted of 12 hours' heating at a particular temperature, followed by a relatively rapid cooling in a flow of air (cooling rate approx. 400 ℃/min). The kinetics of the cyclic oxidation was monitored by weighing the samples after each oxidation cycle, and also by measuring the scale thickness.

The cross-sectional morphology, phase and chemical composition of the scales were studied using optical microscopy, scanning electron microscopy (SEM) with wave dispersion spectrometry (WDS) and energy dispersion spectrometry (EDS) (Jeol JXA 733), and X-ray diffraction analysis (XRD) (X'Pert Philips).

3. Results and discussion

3.1 As-cast microstructure and phase composition

The microstructure of the as-cast TiSi8 alloy is shown in Fig. 2a. Since the chemical composition of the alloy is hypoeutectic, see Table 1, small primary dendrites of prior β(Ti) can be observed. Upon cooling, the β(Ti) phase is transformed to α(Ti). The eutectic mixture is composed of an α(Ti) matrix and a Ti_5Si_3 silicide. Lamellar, rod-shaped, as well as interconnected silicide particles are present. The phase composition of the alloy (α(Ti) + Ti_5Si_3) is also confirmed by XRD patterns shown in Fig. 3. The presence of the Ti_3Si phase is not proved, so it seems useful to compare the thermodynamic stability of the Ti_3Si and Ti_5Si_3 silicides. The Gibbs energy of formation at three temperatures is shown in Table 2. These data

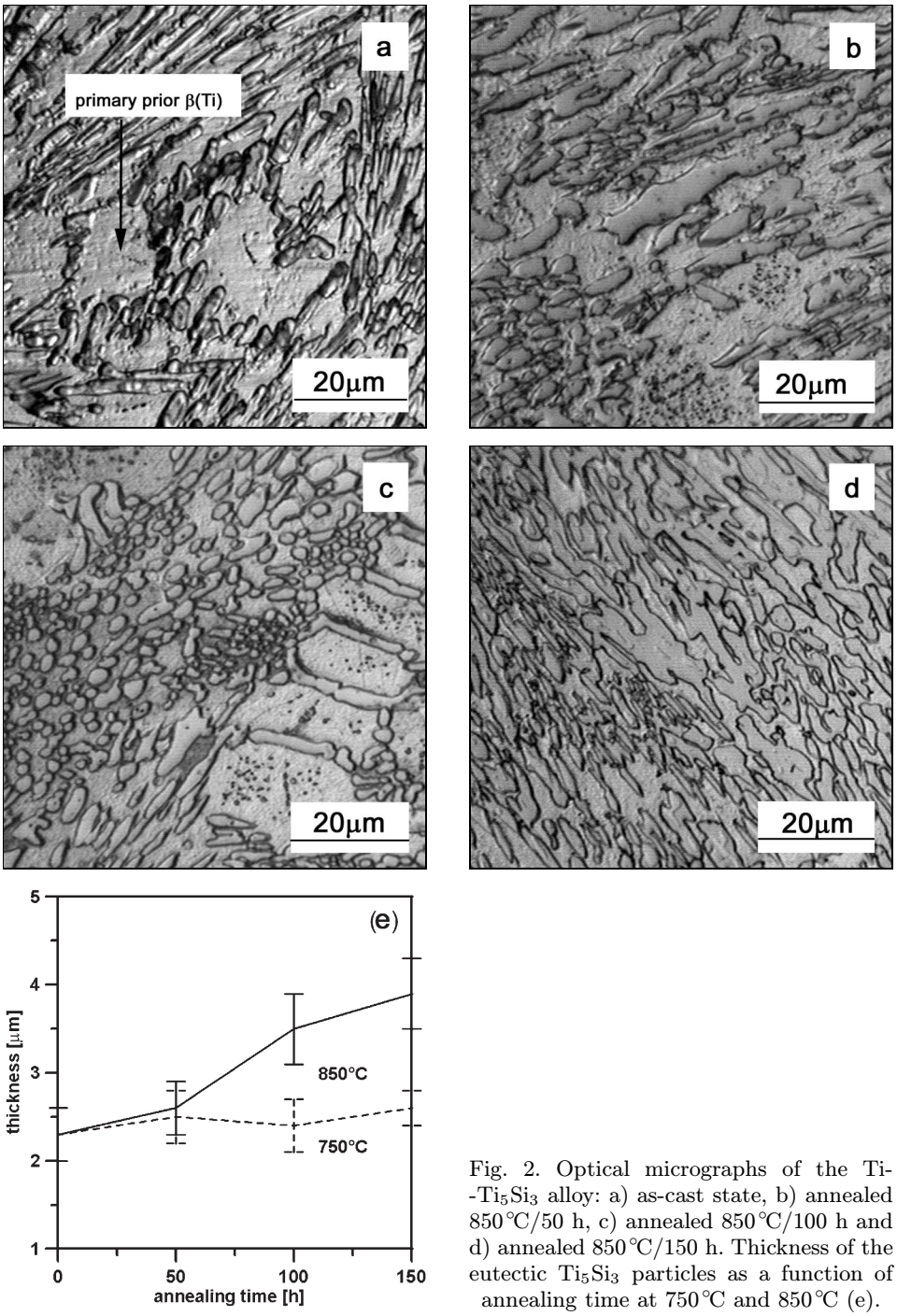

Fig. 2. Optical micrographs of the Ti--Ti_5Si_3 alloy: a) as-cast state, b) annealed 850 °C/50 h, c) annealed 850 °C/100 h and d) annealed 850 °C/150 h. Thickness of the eutectic Ti_5Si_3 particles as a function of annealing time at 750 °C and 850 °C (e).

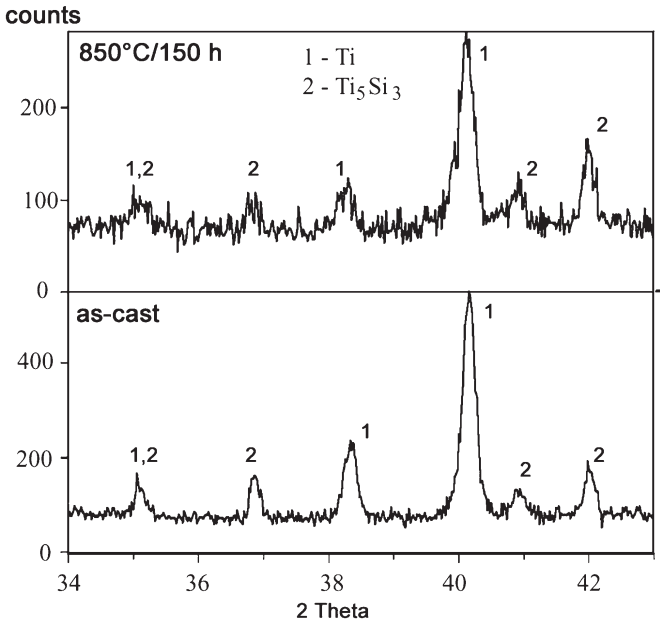

Fig. 3. XRD patterns of the Ti-Ti_5Si_3 alloy in the as-cast state and after annealing at 850 °C/150 h.

Table 2. Gibbs energy of formation ΔG_f^0 of the Ti_5Si_3 and Ti_3Si phases at various temperatures [21, 22]

Temperature [°C]	ΔG_f^0 [kJ/mol]	
	Ti_5Si_3 [21]	Ti_3Si [22]
527	−73.26	−75.78
850	−73.57	−79.48
1027	−73.63	−81.53

show a slightly higher thermodynamic stability of the Ti_3Si phase as compared with the Ti_5Si_3 phase, and thus they do not explain the absence of the former phase. This absence may be explained on the basis of the solid phase transformation kinetics. As shown in Fig. 1, the Ti_3Si phase forms from the Ti_5Si_3 phase through a peritectic reaction at 1170 °C. Upon cooling, this reaction can be written as $Ti + Ti_5Si_3 \rightarrow Ti_3Si$. We may assume that it occurs at the Ti/Ti_5Si_3 interface, with a thin layer of the reaction product being formed. Despite the similarity of lattice parameters c of both silicides, see Table 3, which may favour the nucleation

Table 3. Crystallographic data of Ti-Si phases [23]

Phase	
formula	crystallographic data
Ti_3Si	*tetragonal* $a = 1.0196$ nm $c = 0.5162$ nm
Ti_5Si_3	*hexagonal* $a = 0.7465$ $c = 0.5162$

of the new phase on the original Ti_5Si_3 phase, the diffusion of Ti and Si atoms through the layer of the reaction product is a process controlling the reaction rate. A limited solid state diffusivity, particularly during the relatively rapid cooling of small castings, is thus an obstacle for the peritectic reaction to occur. In fact, no Ti_3Si phase layers were identified either metallographically or by XRD. Besides the kinetic factor, there is another reason for the absence of the Ti_3Si phase, and that is carbon. Pieraggi et al. [24] reports that carbon stabilizes the Ti_5Si_3 silicide. The chemical analysis of the castings proved approx. 0.4 wt.% C which originated from the graphite crucible, see Table 1. This contamination can be considered one of the reasons for the observed stability of the phase composition during annealing, as shown below.

3.2 Changes induced by high-temperature exposition

The stability of the alloy during long-term annealing (150 h) was investigated by way of a metallographic examination, hardness measurement and XRD. The microstructure as a function of the annealing time at 850 ℃ is shown in Figs. 2a–d. It can be seen that the main processes occurring due to annealing are: (i) coarsening of the eutectic Ti_5Si_3 silicide and (ii) precipitation.

The coarsening is driven by the alloy tending to achieve a minimum of interfacial energy. It can be easily monitored by measuring the thickness of the elongated eutectic particles, as shown in Fig. 2e. We can see that the coarsening of the eutectic particles is very slow, which illustrates a high structural stability of the eutectic Ti-Ti_5Si_3 composite. At 850 ℃, the original average particle thickness of 2 μm increases only by less than 2 μm after 150 h annealing. The final structure still contains elongated particles of the Ti_5Si_3 silicide, see Fig. 2d. The annealing at 750 ℃ for 150 h leads to negligible structural changes.

The other process – precipitation – occurs as early as during the first 50 hours of annealing. The precipitates are distinguishable in Figs. 2b,c as fine dark spots dispersed mainly in primary dendrites. These precipitates form a hexagonal Ti_5Si_3

phase, which is nucleated preferentially on the dislocation substructure of titanium [25]. The Ti_5Si_3 phase was also identified in the annealed alloy by XRD, see Fig. 3. Chumbley et al. [25] investigated precipitates formed during the annealing of an as-quenched Ti-Si alloy. In our case, however, the supersaturated solid solution was formed as early as during the casting. The small casting diameter caused rapid cooling of the alloy. The decomposition of the supersaturated solid solution produced finely dispersed rod-shaped silicides, which shared a 2-fold axis of symmetry with an as-quenched matrix [25].

The XRD patterns of the as-cast alloy and that of the alloy annealed at 850 ℃ for 150 h are shown in Fig. 3. The XRD does not prove any phase transformation induced by the high temperature exposition. The high thermal stability of the Ti_5Si_3 silicide does not agree with the results reported by Pieraggi [24], who observed the total transformation of the Ti_5Si_3 phase into the Ti_3Si phase due to annealing at 840 ℃ for 400 hours. The same authors, however, reported the stabilizing effect of carbon on the Ti_5Si_3 silicide by way of the formation of a $Ti_5Si_3C_X$ ($X < 0.3$) phase. Given the above statement and the high affinity of C to Ti, we may assume that the carbon present in the amount of approx. 0.4 wt.%, see Table 1, is more concentrated in the Ti_5Si_3 phase. Small carbon atoms may be incorporated in the interstitial positions of the silicide lattice, thus increasing the number of strong Ti-C bonds and the stability of the silicide.

The slow structural changes illustrated in Figs. 2a–e are in good agreement with the time dependence of hardness as illustrated in Figs. 4a,b. The hardness of the alloy in the as-cast state is relatively high (approx. 550 HV 5) due to a number of eutectic silicide particles dispersed in the microstructure. These particles are rod-shaped, lamellar or interconnected, see Fig. 2a, and they do not exhibit any plastic deformation under loading. The original supersaturation of the solid solution is another contribution to the hardness of the as-cast alloy. This supersaturation is proved by the precipitation observed during annealing, see Figs. 2b,c, as shown earlier. Silicon is known to be an effective strengthening agent in a solid solution as it segregates on dislocations and reduces their mobility even at elevated temperatures [13]. Figures 4a,b also show hardness reducing very slowly during annealing at 750–850 ℃. This illustrates the high structural stability of the Ti-Ti_5Si_3 eutectic composite. There may be two reasons for the hardness reduction which were already described above: (i) the coarsening of eutectic silicides, see Figs. 2a–e, and (ii) the reduction of the solid solution supersaturation accompanied by precipitation, see Figs. 2b,c. The precipitation itself may contribute to hardening, but this contribution is probably small as the precipitates are relatively coarse. This is confirmed by the fact that they are distinguishable by optical microscopy, and also by the results presented in [25] where the rod-shaped precipitates formed at 750 ℃ for 24 hours are nearly 1 micron long. A higher hardening response might be observed at lower temperatures and shorter annealing times.

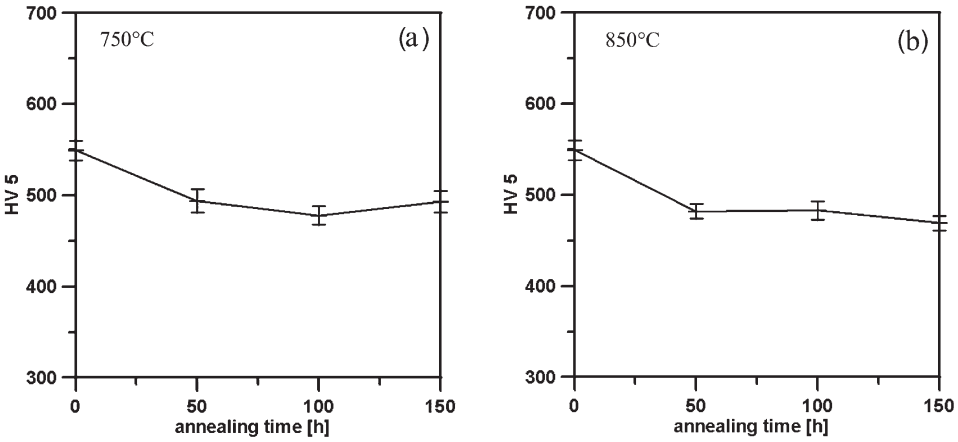

Fig. 4. Hardness HV 5 as a function of annealing time at: a) 750 °C and b) 850 °C.

3.3 Cyclic oxidation kinetics

The plots of the weight gains versus the oxidation time for the Ti-Ti_5Si_3 alloy and for pure Ti are shown in Figs. 5a–c. Cyclic oxidation is generally characterized by a mass growth due to oxidation, and by scales spallation. In our case, however, no spallation was observed, not even in the case of pure Ti and at 1050 °C. This was most likely due to the limited length of oxidation experiments and to very careful manipulation with the samples. Hence, the weight gains in Figs. 5a–c reflect the total amount of CO_2 reacting with the metal. It can be seen that the mass growth due to the reaction is much more rapid in the case of pure titanium. The presence of Ti_5Si_3 strongly reduces the cyclic oxidation rate even at a very high temperature of 1050 °C. At 850 °C and 950 °C, the silicide reduces the total weight gain more than 10 times as compared with pure Ti. At 1050 °C, the total weight gain for the Ti-Ti_5Si_3 alloy is still four times lower as compared with pure Ti. The protective effect of the silicide during temperature cycling thus appears to be better at a lower temperature.

The different oxidation behaviour of the investigated materials is also illustrated in Figs. 6a,b and 7a–c, which show cross-sections of their scales. The average scale thickness after the total oxidation period is listed in Table 4. The results confirm the strong protective effect of the silicide. It should be noted, however, that the data in Table 4 are not in full agreement with those shown in Figs. 5a–c. The scales on pure titanium are 14 times, 19 times and 9 times thicker than those on the Ti-Ti_5Si_3 alloy after oxidation at 850, 950 and 1050 °C, respectively. This discrepancy is caused by the presence of porosity in the scales. The porosity is developed mainly on pure Ti, but it can be also observed on the Ti-Ti_5Si_3 alloy oxidized at

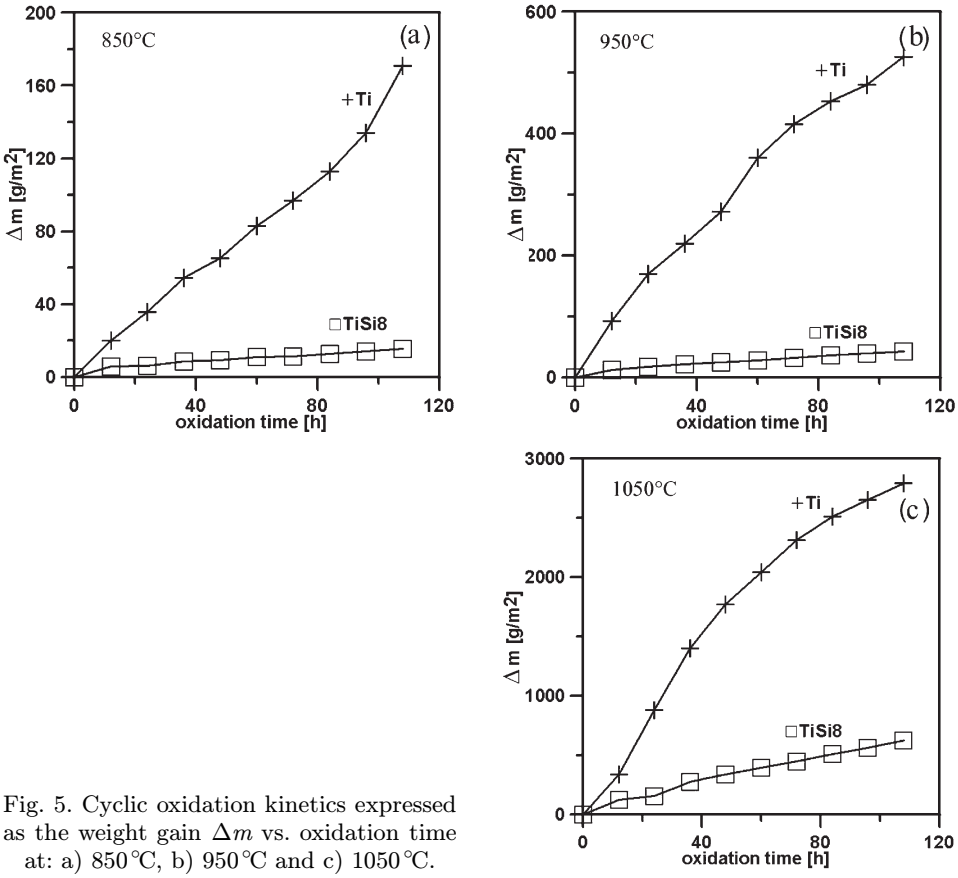

Fig. 5. Cyclic oxidation kinetics expressed as the weight gain Δm vs. oxidation time at: a) 850 °C, b) 950 °C and c) 1050 °C.

Table 4. Average scale thickness after 108-h cyclic oxidation at 850–1050 °C in CO_2

Alloy	Scale thickness [μm]		
	850 °C/108 h	950 °C/108 h	1050 °C/108 h
Ti	110	320	1800
Ti-Ti_5Si_3	8	17	190

1050 °C, see Fig. 7c. The porosity results in a considerable growth of the scales volume. The pores are believed to result from CO_2 and CO gases, which penetrate through the scales. The CO gas is formed near the scale/metal interface by the reaction of the metal with CO_2. Normally, such gases are in the atomic state and are transported in the rutile lattice by diffusion. On structural defects, however, the C and O atoms may recombine to form CO and CO_2. As a result, pores are formed which eventually facilitate CO_2 penetration towards the metallic substrate.

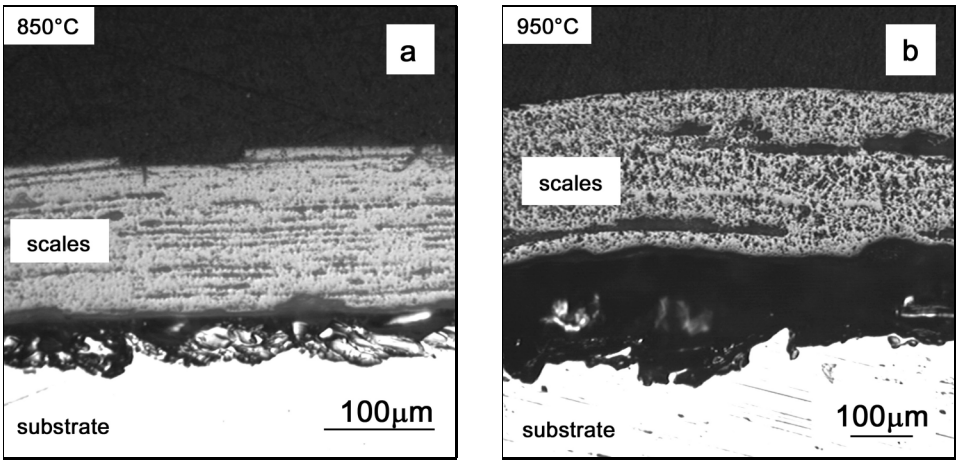

Fig. 6. Optical micrographs of cross-sectional scales on the pure Ti after 108 h cyclic oxidation in CO_2 at: a) 850 °C and b) 950 °C.

The higher volume fraction of porosity observed for pure Ti is in accordance with thick scales of poor adherence to the metallic substrate.

In order to determine the protective effect of scales formed during the initial stage of oxidation against further oxidation, a detailed investigation of the kinetic curves shown in Figs. 5a–c is needed. If the scales are compact, non-porous, non--cracked, the oxidation is mostly governed by the diffusion of species through them. The oxidation rate progressively reduces with the oxidation time and such scales are regarded as well protecting. On the other hand, if pores and/or cracks are present in the scales, the oxidizing agents penetrate easily towards the metallic substrate. Such scales provide only a slight protection against oxidation. In the former case, the general parabolic law is mostly applied:

$$\Delta m^2 = K_{\mathrm{P}} \cdot \tau, \tag{1}$$

where Δm, K_{P} and τ stand for the weight gain, parabolic rate constant and time, respectively. In general, this law is applied for isothermal oxidation. Assuming that cyclic oxidation is not accompanied with any scale spallation, we may consider this law, too. If we want to decide whether or not the parabolic law is valid, it seems reasonable to compute the parabolic rate constant K_{P} at each point of the kinetic curves in Figs. 5a–c using Eq. (1). If the rate constant does not vary during the oxidation, the parabolic law is valid. Since the rate constants vary within a range of several orders of magnitude, we computed a $K_{\mathrm{P}}/K_{\mathrm{P1}}$ ratio, where K_{P1} is the

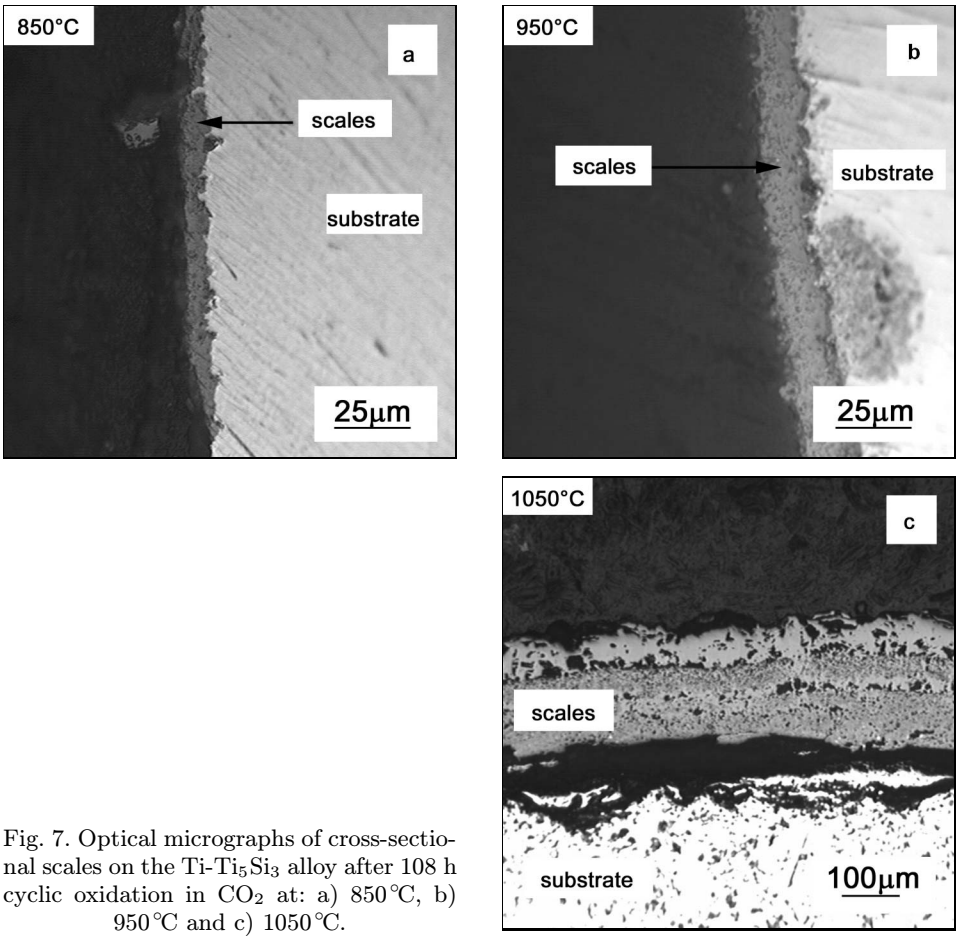

Fig. 7. Optical micrographs of cross-sectional scales on the Ti-Ti_5Si_3 alloy after 108 h cyclic oxidation in CO_2 at: a) 850 °C, b) 950 °C and c) 1050 °C.

Table 5. Parabolic rate constants K_{P1} corresponding to 12 h oxidation

Alloy	K_{P1} [$g^2 \cdot m^{-4} \cdot ks$]		
	850 °C	950 °C	1050 °C
Ti	9.20	198	2610
Ti-Ti_5Si_3	0.740	3.50	366

value corresponding to 12 hours' oxidation. The values of K_{P1} are listed in Table 5, and the K_P/K_{P1} ratio as a function of the oxidation time is plotted in Figs. 8a,b.

For pure Ti we can observe in Fig. 8a that the rate constant grows with the oxidation time at all temperatures. The K_P values after the last oxidation period are almost eight times higher than those after the first period of oxidation (K_{P1}). This is not surprising because it is well known that the parabolic law does not reflect

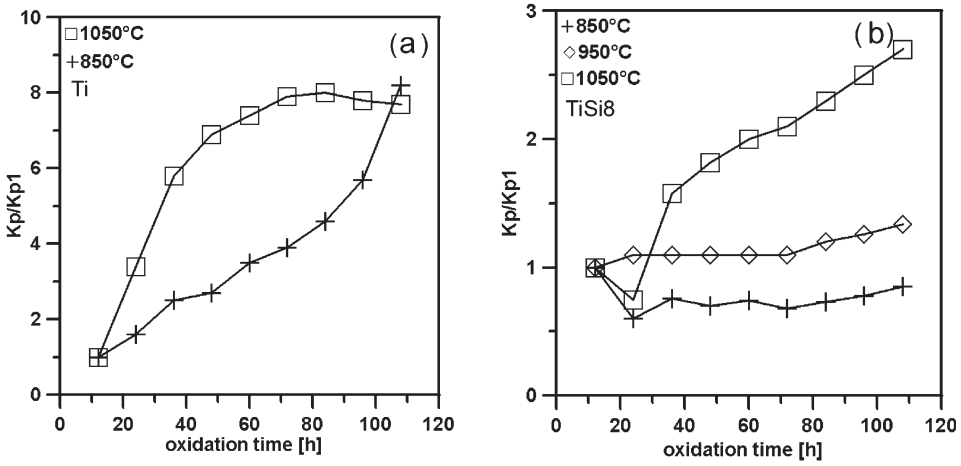

Fig. 8. K_P/K_{P1} ratio of the pure Ti (a) and the Ti-Ti_5Si_3 alloy (b) as a function of the oxidation time.

the real oxidation behaviour of pure titanium. The scales formed due to oxidation are not a very efficient protective barrier preventing any further penetration of CO_2, and, consequently, diffusion is not the process governing the oxidation. This is also in agreement with the high fraction of scale porosity and large thickness of the scales, see Table 4 and Figs. 6a,b.

The K_P/K_{P1} ratio plotted in Fig. 8b represents the Ti-Ti_5Si_3 alloy oxidized at 850–1050 ℃. Here the behaviour is quite different from that of titanium. The K_P/K_{P1} values at 850 and 950 ℃ stay at approx. the same level close to unity for the whole experimental period. No significant trend of their increase or decrease with time can be observed. Small deviations may be attributed to possible experimental errors in our measurements. This means that the parabolic law is a good approach to the cyclic oxidation behaviour of the Ti-Ti_5Si_3 alloy at 850–950 ℃ for up to 108 hours, and that diffusion through scales governs the oxidation. Indeed, the scales shown in Figs. 7a,b are dense, compact and adherent to the substrate, despite the thermal cycling, thus providing a good barrier against CO_2 penetration. At 1050 ℃, however, see Fig. 8b, this conclusion no longer applies, and the K_P/K_{P1} values rise progressively with the oxidation time. This implies that the protective effect of the scales on the Ti-Ti_5Si_3 alloy is reduced at 1050 ℃. The optical micrograph in Fig. 7c reveals that such behaviour results from the porosity in the scales and from their poor adherence to the substrate. High temperature combined with thermal cycling seems to provide good conditions for the formation of structural defects and porosity in the scales.

3.4 Chemical and phase composition of scales

The scales formed on both investigated materials at all temperatures were analysed by XRD. The only phase identified was rutile, as illustrated on XRD patterns in Fig. 9. Neither silica nor any lower titanium oxides were detected. The concentration profiles of chemical elements were measured on cross-sectional scales, and the results for the temperature of 1050 ℃ are shown in Figs. 10a,b.

In the case of pure Ti, the distribution of Ti and O is almost uniform across the scales and corresponds to rutile (40 wt.% O), see Fig. 10a. The locally decreased concentrations of both elements correspond to the pores, where the analysed signal reduces. The scales are also characterized by an almost constant concentration of nitrogen (a few wt.%), which originates from impurities in the CO_2 used. In the titanium matrix just beneath the scales, oxygen and nitrogen concentrations achieve several wt.%. The atoms of these elements occupy the interstitial positions in the Ti lattice to form a solid solution. The presence of interstitials in the Ti lattice leads to a significant hardening and strengthening of titanium. Carbon is not proved either in the scales or in the metallic substrate, hence the reaction of Ti with CO_2 can be written as

$$\mathrm{Ti(s)} + 2\mathrm{CO_2(g)} \rightarrow \mathrm{TiO_2(s)} + 2\mathrm{CO(g)}. \quad (2)$$

This reaction is favoured thermodynamically since the Gibbs energy ΔG^0 is −318 kJ/mol, −310 kJ/mol and −302 kJ/mol at 850 ℃, 950 ℃ and 1050 ℃, respectively.

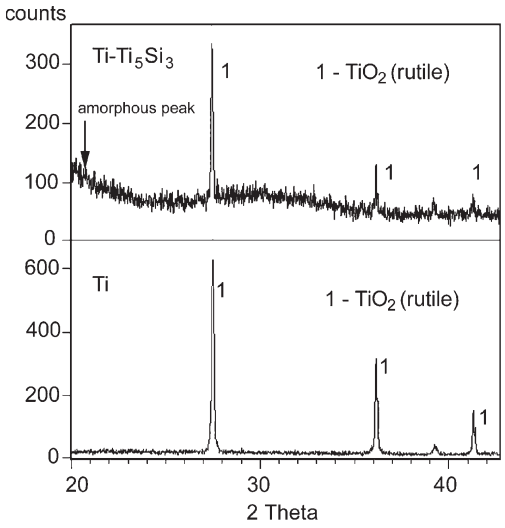

Fig. 9. XRD patterns of the scales on the pure Ti and the Ti-Ti_5Si_3 alloy oxidized in CO_2 at 1050 ℃ for 108 h.

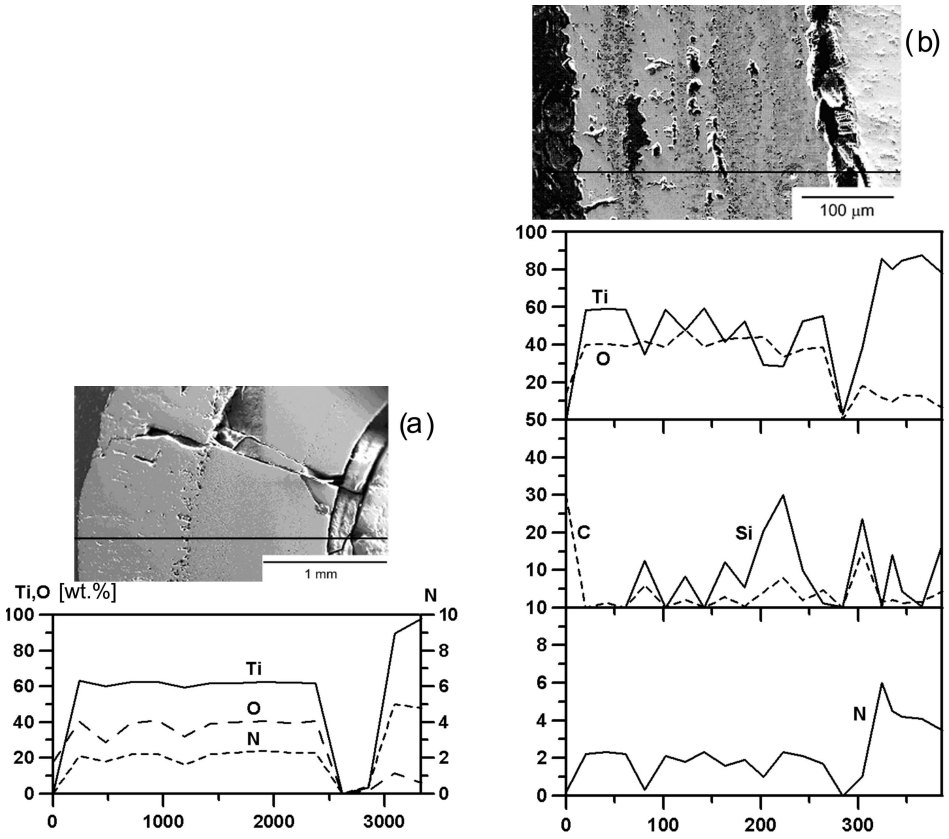

Fig. 10. The concentration [wt.%] profiles of chemical elements in the cross-sectional scales on the pure Ti (a) and the Ti-Ti_5Si_3 alloy (b) oxidized in CO_2 at 1050 °C for 108 h.

The oxidation of titanium is known to occur at the oxide/metal interface and is thus governed by the penetration of the oxidizing medium through the scales. The dissociation of CO_2 into CO and O is probably the first step of the reaction. The atomic oxygen then reacts with Ti to form a new layer of TiO_2 at the oxide/metal interface, and partly diffuses into the metal to form an interstitial solid solution. The reaction product, carbon monoxide, is then transported outwards the scales both in the atomic state by diffusion and in the gaseous state by cracks and pores, see Fig. 10a. Since we detected a negligible carbon concentration in the scales, the latter mechanism seems to predominate and the gaseous CO may be the reason for cracking of the scales as observed in some locations, see Fig. 10a. Another reason for the cracking may be the thermal cycling, which induces stress in the scales. As the scales are cooled in the flow of air, a temperature gradient forms within

them. The outer parts of the scales tend to contract while the inner parts remain unchanged. As a consequence, tensile and pressure stress is induced in the outer and inner parts of the scales, respectively. The stress leads to the formation of cracks which are perpendicular to the surface of the substrate, see Fig. 10a. In the case of thin scales (the Ti-Ti_5Si_3 alloy, see Figs. 7a–c), the temperature differences are small and not sufficient to cause any cracking.

The distribution of Ti, O, N, C and Si in the scales formed on the Ti-Ti_5Si_3 alloy at 1050 ℃ is shown in Fig. 10b. Just as in the preceding case, the scales contain almost uniformly distributed oxygen in the amount of approx. 40 wt.%, which corresponds to rutile as the major component of the scales, see also Fig. 9. In addition to oxygen, nitrogen is also uniformly distributed across the scales in the amount of a few wt.%. Similarly as in the case of pure Ti, the components of the oxidizing atmosphere are not concentrated only in the scales, but they also penetrate into the metallic substrate of the Ti-Ti_5Si_3 alloy to form an interstitial solid solution. Besides rutile, however, some other phases can be recognized in the scales as indicated by the non-uniform distribution of Ti and Si. The sites of an increased Si concentration and decreased Ti concentration correspond to the particles of the Ti_5Si_3 silicide in the original microstructure. The high oxygen content at these sites implies that rutile and silica are the main components in these locations. Their formation can be described by the equation:

$$Ti_5Si_3 + 16CO_2 \rightarrow 5TiO_2 + 3SiO_2 + 16CO. \quad (3)$$

Even though silica was not detected in our experiment by XRD, see Fig. 9, its occurrence in the scales on the oxidized Ti-Si alloys has been proved in a number of papers [17, 19]. In addition, the reaction (3) is thermodynamically favoured since ΔG^0 at 1050 ℃ is −2280 kJ/mol. The absence of silicon dioxide in the XRD pattern can be attributed to its amorphous nature [17, 19], as indicated by an amorphous peak at low 2 Theta angles in Fig. 9. The absence of silicon in the outer part of the scales, as also schematically shown in Fig. 11, is believed to result from: (i) slightly higher thermodynamic stability of TiO_2 as compared with SiO_2 [21], (ii) preferential reaction of the oxidizing agent with Ti due to its higher activity (silicon is fixed in the stable silicide), and (iii) relative immobility of Si atoms in the scales, which is consistent with the higher bond energy of Si^{4+}—O (465 kJ/mol) as compared with Ti^{4+}—O (323 kJ/mol) [26]. The diffusion of titanium atoms in the scales towards their surface thus seems to occur during oxidation, even though it is generally believed that oxidation is governed primarily by the inward diffusion of the oxidizing agent [17].

The presence of Si (SiO_2) in the scales has a considerable effect on the oxidation rate, see Figs. 5a–c: Firstly, silicon strongly slows down the diffusion rate of species in the oxide scales by reducing the concentration of vacancies responsible for

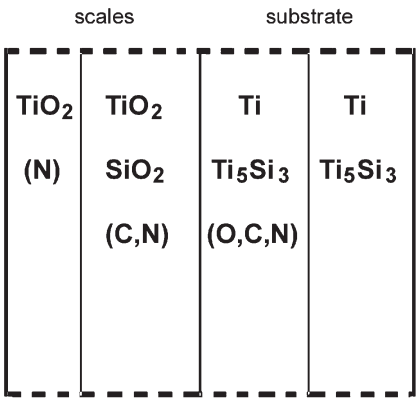

Fig. 11. Schematic sketch of the internal substructure of the scales formed on the Ti-Ti_5Si_3 alloy oxidized in CO_2.

diffusion [19]. The reduced diffusion flow of atoms through the scales also results in a reduced porosity of the scales, compare Figs. 6a and 7a. Secondly, silicon hinders any deep penetration of interstitials into the metallic substrate [18]. This can be attributed both to the reduced diffusion rate and to the reduced solubility of the interstitials in Ti. Thirdly, fine silica particles in the scales support the formation of a finely grained rutile structure. Such a structure contains a lower amount of defects like microcracks because it is able to better resist stresses induced by thermal cycling. The grain boundary diffusion creep is the main mechanism of stress relief [17]. The finely grained structure is generally characteristic of dense, compact and adherent layers, as in our case.

In addition to silica, there is another difference between the Ti-Ti_5Si_3 alloy and pure titanium, the presence of carbon. This element was detected in the scales on the Ti-Ti_5Si_3 alloy in an amount of up to several wt.%, see Fig. 10b. Its distribution was non-uniform as it was concentrated mainly at the sites enriched with Si, see also Fig. 11. This means that part of the silicide reacts with CO_2 and/or CO to form carbon-containing products. Most probably these products are based on amorphous $SiC_XO_{2(1-X)}$ phase. Others products, like e.g. solid solutions of C in TiO_2 or in lower Ti oxides, δ (TiC-TiO), TiC or SiC can also be considered, according to the Ti-C-O and Si-C-O phase diagrams [27–29]. The chemical microanalysis proved the presence of carbon not only in the scales but also in the metallic substrate, probably in the form of an interstitial solid solution. This means that silicon increases the susceptibility of titanium to the reaction with carbon contained in CO_2, despite the overall reduction of the oxidation rate. When the dissociation of CO_2 into CO and O occurs, atomic oxygen is consumed preferentially by the oxidation of the Ti matrix to form very stable TiO_2. The remaining oxygen then reacts with the silicide to form TiO_2 and SiO_2, see Eq. (3). As the thermodynamic stability of the silicide Ti_5Si_3 is lower than that of TiO_2 and SiO_2, see Table 6, the reaction of CO

Table 6. Gibbs energy of formation ΔG_f^0 of the Ti_5Si_3, TiO_2 and SiO_2 at 850 and 1050 °C [21]

Temperature [°C]	ΔG_f^0 [kJ/mol]		
	Ti_5Si_3	TiO_2	SiO_2
850	−74	−247	−236
1050	−74	−235	−226

with the remaining silicide may occur to form some of the C-containing products which were suggested above. In the case of pure Ti, on the other hand, the scales contain only stable rutile and no other reaction with CO occurs at the testing temperatures. The reaction of CO with TiO_2 producing, e.g., δ (TiC-TiO) might perhaps proceed at much higher temperatures [30, 31].

4. Summary

The most important results of this work documenting some aspects of the high-temperature behaviour of the Ti-Ti_5Si_3 alloy can be summarized as follows:

1. The as-cast TiSi8 alloy is an in situ eutectic composite consisting of Ti and Ti_5Si_3 phases. The Ti_3Si phase has not been found due to the kinetic factor and the presence of carbon.

2. The high-temperature exposition induces slow coarsening of the eutectic Ti_5Si_3 silicide and the precipitation of the Ti_5Si_3 silicide from a supersaturated solid solution. No phase transformation, e.g. into Ti_3Si, has been detected, which is consistent with the stabilizing effect of carbon. The structural changes are accompanied with a very slow hardness reduction.

3. Measurements of the oxidation kinetics have proved the strong protective effect of the Ti_5Si_3 silicide. The slow oxidation of Ti-Ti_5Si_3 at 850–950 °C is governed by diffusion through scales, and is described by the parabolic law. In the case of pure Ti and the Ti-Ti_5Si_3 alloy oxidized at 1050 °C, the parabolic law does not apply as the scales are porous, cracked, and characterized by poor adherence to the substrate.

4. The main component of the scales on both tested materials is rutile. The scales on the Ti-Ti_5Si_3 alloy also contain amorphous silica with a small amount of carbon, with the silica originating from the Ti_5Si_3 silicide oxidation.

Acknowledgements

This work was part of research programme MSM 6046137302, and it was also financially supported by the Academy of Sciences of the Czech Republic under project No. IAA1010414.

REFERENCES

[1] LEYENS, C.—PETERS, M.: Titanium and Titanium Alloys, Fundamentals and Applications. Weinheim, Wiley-VCH 2003.
[2] HARDING, R. A.: Kovove Mater., *42*, 2004, p. 225.
[3] LAPIN, J.—PELACHOVÁ, T.: Kovove Mater., *42*, 2004, p. 143.
[4] LAPIN, J.—KLIMOVÁ, A.: Kovove Mater., *41*, 2003, p. 1.
[5] LAPIN, J.—ONDRÚŠ, Ľ.: Kovove Mater., *40*, 2002, p. 161.
[6] Binary Alloy Phase Diagrams. ASM, Metals Park, OH 1986.
[7] ZHU, J.—KAMIYA, A.—YAMADA, T.—WATAZU, A.—SHI, W.—NAGANUMA, K.: Mat. Trans., *42*, 2001, p. 336.
[8] SAHA, R. L.—NANDY, T. K.—MISRA, R. D. K.: Scripta Metall., *23*, 1989, p. 81.
[9] LAVELLE, B.—DABOSI, F.: In: Proceedings Titanium 80. Eds.: Kimura, H., Izumi, O. Warrendale, The Met. Soc. AIME 1980, p. 2275.
[10] HANSEN, M.: Constitution of Binary Alloys. New York, McGraw-Hill Book Company 1958.
[11] MAZUR, V. I.—SUKHIKH, L. L.—FIRSTOV, S. A.—KULAK, L. D.: In: Proceedings Processing, Properties and Applications of Metallic and Ceramic Materials. Eds.: Loretto, M. H., Beevers, C. J. Vol. 1. Birmingham, EMAS 1992, p. 141.
[12] DONG, H.—BLOYCE, A.—MORTON, P. H.—BELL, T.: In: Proceedings Titanium 95. Warrendale, The Met. Soc. AIME 1995, p. 2007.
[13] WINSTONE, M. R.—RAWLINGS, R. D.—WEST, D. R. F.: J. Less Common Met., *39*, 1975, p. 205.
[14] NAKA, M.—MATSUI, T.—MAEDA, M.—MORI, H.: Mat. Trans. JIM., *36*, 1995, p. 797.
[15] SURYANARAYANA, C.—INOUE, A.—MASUMOTO, T.: J. Mat. Sci., *15*, 1980, p. 1993.
[16] DONG, H.—LI, X. Y.—BELL, T.: J. Alloy Compd., *283*, 1999, p. 231.
[17] LEE, D. B.—PARK, K. B.—JEONG, H. W.—KIM, S. E.: Mat. Sci. Eng., *A328*, 2002, p. 161.
[18] CHAZE, A. M.—CODDET, C.: J. Mat. Sci., *22*, 1987, p. 1206.
[19] CHAZE, A. M.—CODDET, C.: Oxid. Met., *27*, 1987, p. 1.
[20] VOJTĚCH, D.—BÁRTOVÁ, B.—KUBATÍK, T.: Mat. Sci. Eng., *A 361*, 2003, p. 50.
[21] BARIN I.: Thermochemical Data of Pure Substances. Weinheim, Wiley-VCH 1993.
[22] VAHLAS, C.—CHEVALIER, P. Y.—BLANQUET, E.: Calphad, *13*, 1989, p. 273.
[23] SVETSCHNIKOV, V. N.—KOTSCHERZINSKIJ, J. A.—JUPKO, L. M.—KULIK, O. G.—SISKIN, J. A.: Doklady Akademii Nauk SSSR, *193*, 1970, p. 393 (in Russian).
[24] PIERAGGI, B.—RAFFY, M.—DABOSI, F.: In: Proceedings Int. Conf. Met. Corros. 84, Ottawa 1984, p. 348.
[25] CHUMBLEY, L. S.—MUDDLE, B. C.—FRASER, H. L.: Acta Metall., *36*, 1988, p. 299.
[26] HABAZAKI, H.—SHIMIZU, K.—NAGATA, S.—SKELDON, P.—THOMPSON, G. E.—WOOD, G. C.: Corros. Sci., *44*, 2002, p. 1047.
[27] VICENS, J.—CHERMANT, J. L.: Revue de Chimie Minerale., *9*, 1972, p. 557.
[28] HASHIMOTO, Y.—OHMORI, S.—KOHYAMA, K.—ARAMI, Y.: Japan. Koon Gakkaishi., *7*, 1981, p. 209.
[29] BREQUEL, H.—BADHEKA, R.—BABONNEAU, F.—ENZO, S.: Journal of Materials Synthesis and Processing, *8*, 2000, p. 369.
[30] KOC, R.: Journal of the European Ceramic Society, *17*, 1997, p. 1309.

[31] GOTOH, Y.—FUJIMURA, K.—KOIKE, M.—OHKOSHI, Y.—NAGURA, M.—AKAMATSU, K.—DEKI, S.: Materials Research Bulletin, *36*, 2001, p. 2263.